

# Influence of Zinc doping on the structural and optical properties of chemically synthesized PbO nanocrystals

N. MYTHILI, K. T. ARULMOZHI<sup>a,\*</sup>

*Department of Physics, Annamalai University, Tamil Nadu-608 002, India*

*<sup>a</sup>Physics wing (DDE), Annamalai University, Tamil Nadu-608 002, India*

Doped semiconductor nanoparticles have greater impact on their structural and optical properties due to quantum size effects. Zn doped PbO nanoparticles are synthesized by chemical precipitation with Lead (II) Acetate and Zinc Acetate Trihydrate as precursors. The synthesized particles are characterized using X-ray diffraction (XRD), Fourier Transform Infrared Spectroscopy (FT-IR), UV-Visible spectroscopy (UV-Vis), Photoluminescence spectroscopy (PL), Field Emission Scanning Electron Microscopy (FESEM) and Energy Dispersive Spectroscopy (EDS), High Resolution Transmission Electron Microscopy (HRTEM). XRD studies reveal that the average crystallites are in the range of 23 and 40 nm and Specific Surface Area (SSA) is also determined. Zn doped PbO Nanocrystals exhibit the blue shift around 250 nm in the absorption spectra and the band gap is around 3.87 eV. FT-IR shows the metal vibrations and EDS spectrum reveals the elemental concentrations. The results imply that Zn doping enhance the structural and optical properties of PbO nanocrystals.

(Received October 2, 2013; accepted March 13, 2014)

*Keywords:* Zn doped PbO, Nanocrystals, Chemical method, Optical-structural properties

## 1. Introduction

Metal oxides are widely used in gas sensing, catalysts, solar cells, information storage [1]. These metal oxide mixtures are also helps in the building blocks of new organic-inorganic hybrid nanostructures. Chemical doping is one of the feasible ways to tailor the metal oxides to suit the applications. Doping of semiconductor with selective elements offers an interesting approach to regulate the structural, optical and electrical properties. Among the mixed metal oxides incorporation of transition metals into lead have attracted broad interest due to the piezoelectric, ferroelectric and photoluminescence properties [2, 3]. Lead monoxide (PbO) is a photo active semiconductor metal oxide and has gained industrial important due to its effective applications. Zinc plays an important role in the applications such as solar cells and optoelectronic devices [4].

Intensive research has been focused on the synthesis of PbO and ZnO nanoparticles and nanocomposite by chemical methods [5, 6,], hydrothermal synthesis [7, 8], and thermal evaporation method [9]. Significant studies have been carried out on the effect of Pb doping into the ZnO matrix [10, 11, 12]. The results indicated modifications in the structural properties of the ZnO nanocrystals, but some with adverse effects. This is due to the fact that Pb has large ionic radius (1.19Å) than Zinc (0.79Å) and the incorporation of Pb into the ZnO lattice will introduce lattice distortion. This leads to the changes in the energy band structure of the ZnO matrix and new/increased defects such as oxygen vacancies etc. [13]. Alternatively, if lighter Zn is doped into the PbO nanostructures one can expect reduced defects and

enhanced optical and electrical properties of the PbO nanocrystallites. With this aim the present work is designed to study the effect of Zn doping on the PbO nanostructure and to bring out the favorable aspects. The results reported are relevant to an optimum concentration of Zn doping.

## 2. Materials and methods

All chemicals used in this study are of AR grade with 99% purity (Merck and SD fine chemicals) and used without further purification. 0.5N of Pb (CH<sub>3</sub>COO)<sub>2</sub>·3H<sub>2</sub>O and 0.1 N of Zn(CH<sub>3</sub>COO)<sub>2</sub>·2H<sub>2</sub>O were dissolved in 100 ml of water and stirred continuously to get a transparent solution. The solution is adjusted to maintain the pH = 9 by adding 9.5N NaOH and stirred for 2 h. The resulting red precipitate obtained was washed with water and ethanol alternatively, filtered and dried at 100 °C for 2 h. The sample was then heat treated at 240°C for about 2 h.

## 3. Instrumentation

The XRD patterns of the powder samples were recorded using X'PERT PRO diffractometer with Cu-Kα radiation (λ=1.5406 Å). The FT-IR spectra were recorded using SHIMADZU-8400 spectrometer using KBr pellet method. The UV-Vis absorption spectra of all samples in Dimethyl sulphoxide (DMSO) were recorded using LAMBA 25 PERKIN ELMER spectrometer. PL spectra study was carried out in PERKIN ELMER LS 55 fluorescence spectrometer. The morphology of the

samples was observed from HITACHI S-4700 FESEM. EDS measurement were carried out with HITACHI S-4700. High-resolution transmission electron microscopy (HRTEM) analysis was performed using JEOL 3010 HRTEM.

## 4. Results and discussion

### 4.1. XRD

The XRD patterns of Zn doped and pure (undoped) PbO nanoparticles are shown in Fig. 1. The diffraction peaks matches with the JCPDS card 05-0561. In the pure PbO the highly intense peak is in the plane (101) whereas, in Zn doped PbO it is (002). Similarly the planes (001), (112) are highly intense when compared to pure PbO. These shifts in plane intensities are due to zinc doping in the PbO matrix. In general the Zn doped PbO pattern show well defined crystallinity and high intensity peaks.

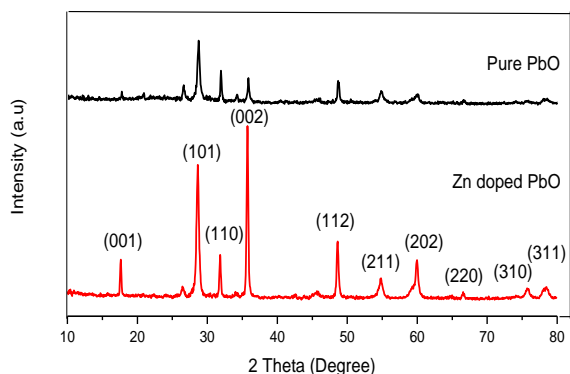


Fig. 1. XRD pattern of pure and Zn doped PbO nanocrystals.

#### 4.1.1. Crystallite size (D)

The crystallite sizes of pure PbO and Zn doped PbO were determined using the scherrer formula [14] and it is given in Table 1.

$$D = \frac{0.9\lambda}{\beta \cos\theta}$$

where D is the mean crystallite size,  $\lambda$  is the wavelength of CuK $\alpha$  line ( $=1.5405\text{\AA}$ ),  $\beta$  is the full width at half maximum (FWHM) and  $\theta$  is Bragg's diffraction angle.

#### 4.1.2 Specific Surface Area (SSA)

SSA is the surface area per unit mass. SSA determines the reactive properties of a material [15] it is calculated using the relation

$$SSA = \frac{SA_{part}}{V_{part} \times Density}$$

Where  $SA_{part}$  is the Surface Area of the particle,  $V_{part}$  is the particle volume and Density is the theoretical density of PbO.

#### 4.1.3. Crystallinity Index ( $I_{cry}$ )

Crystallinity refers to the degree of structural order in a solid. Crystallinity can be measured using XRD. It is evaluated through comparison of crystallite size obtained from XRD data and that ascertained by TEM/SEM. The crystallinity Index ( $I_{cry}$ ) can be calculated using the relation

$$I_{cry} = D_p / D$$

where  $D_p$  is the particle size obtained from SEM/TEM and D is the particle size calculated using Scherrer formula. When  $I_{cry}$  is close to 1, it is assumed that the crystallite size represents monocrystalline units. Much larger value of  $I_{cry}$  means the particles are of polycrystalline type. The calculated parameters are given in Table 1.

Table 1. Parameters calculated from the XRD analysis.

| Sample       | Crystallite size (D) (nm) | Specific Surface Area (SSA) ( $\text{m}^2 \text{g}^{-1}$ ) | Crystallinity Index ( $I_{cry}$ ) |
|--------------|---------------------------|--|-----------------------------------|
| Pure PbO     | 40                        | 17.58  | 1.9                               |
| Zn doped PbO | 23                        | 27.53  | 1.5                               |

### 4.2 FT-IR

The FT-IR spectra of pure PbO and Zn doped PbO nanoparticles are shown in Fig. 2.

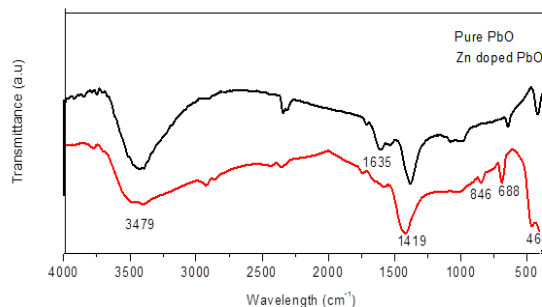


Fig. 2. FT-IR spectrum of pure and Zn doped PbO nanocrystals.

In both spectra the band at  $3479 \text{ cm}^{-1}$  is the characteristic peak of OH stretching vibrations. The band at  $1635 \text{ cm}^{-1}$  is due to the O-H bending vibration of

adsorbed water. The strong and intense peaks around  $1419\text{ cm}^{-1}$  are due to vibration of oxygen with Pb [16]. Absorption peaks around  $846$  and  $462\text{ cm}^{-1}$  are due to metal and metal-oxygen vibrations possibly Zn and Pb-O [17]. A sharp peak around  $687\text{ cm}^{-1}$  represents the asymmetric bending vibration of Pb-O-Pb bond. This peak is more intense in the case of Zn doped PbO. This in turn indicates that zinc doping increases the peak intensity of lead oxide in the sample, which means higher yield of the nanoparticles.

### 4.3. UV-Vis

UV-Vis absorption analysis is an important tool in the characterization of nanoparticles in optical aspects. The absorption maximum of pure PbO is  $273\text{ nm}$  and for the Zn doped is  $250\text{ nm}$  are shown in Fig. 3a. There is a blue shift of Zn doped PbO peak due to the quantum size effect [18]. The calculated band gap is slightly higher for Zn doped PbO nanoparticles as shown in Fig. 3b. It implies the concept that the band gap increases when the particle size decreases [19]

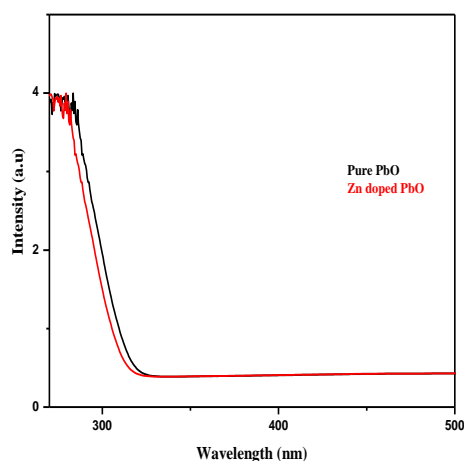


Fig. 3a. UV-Vis absorption spectrum of Pure and Zn doped PbO nanocrystals.

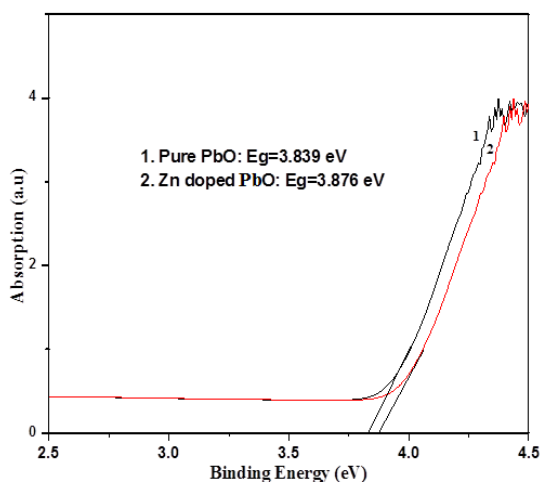


Fig. 3b. Band gap spectrum of pure and Zn doped nanoparticles.

### 4.4. Photoluminescence

PL study is a powerful method for investigating the defects on the nanostructures. Fig. 4 shows the PL emission spectrum of pure and Zn doped PbO nanocrystals. PL spectrum was measured with the excitation wavelength of  $280\text{ nm}$  at room temperature.

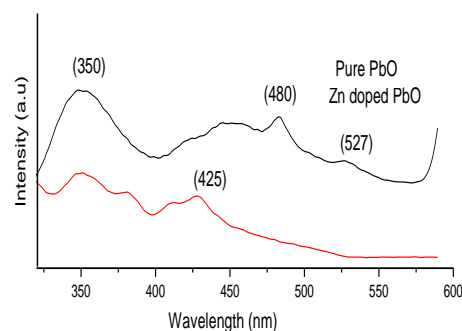


Fig. 4. PL emission spectrum of Pure and Zn doped PbO nanocrystals.

The undoped PbO exhibits a strong ultraviolet band around  $350\text{ nm}$ . In case of Zn doped PbO this peak is less intense and modified due to the exchange of interactions between the band electrons of PbO and the localized 'd' electrons of Zn ions [19]. The weak emission bands around  $410\text{--}455\text{ nm}$  are due to blue emission and it is generally related to the defects like surface traps in the nanocrystals. In undoped PbO spectrum the peak around  $480\text{ nm}$  is the green emission in the visible region indicating the oxygen vacancy defects in the PbO interstitials. This green emission is very low in the case of Zn doped PbO implying the reduced defects. The weak emission peak around  $550\text{ nm}$  in the pure PbO is related to the oxygen vacancies is totally absent in the Zn doped PbO spectrum. Since Zinc had smaller ionic radius than lead, the incorporation of Zn into the PbO lattice may not cause much lattice distortion. This is the reason for the small oxygen defects in the structure.

### 4.5. FE-SEM, EDS

It shows that the Zn doped clearly indicates the spherical formation of particles whereas the pure PbO shows the agglomeration with particles. The average particles are in the range of  $35\text{--}40\text{ nm}$  for Zn doped PbO nanoparticles. EDS spectrum Zn doped PbO nanoparticles is shown in Fig. 4c, which reveals well defined peaks identified as characteristic peaks of Zn, Pb and O confirming that the synthesized nanoparticles are Zn doped lead oxide. This result suggests that zinc doping increases the crystallinity of the particles, which fact is in good agreement with the XRD analysis. The FESEM image of pure and Zn doped PbO are given Fig. 5a and 5b and its corresponding EDS spectrum is given in Fig. 5c.

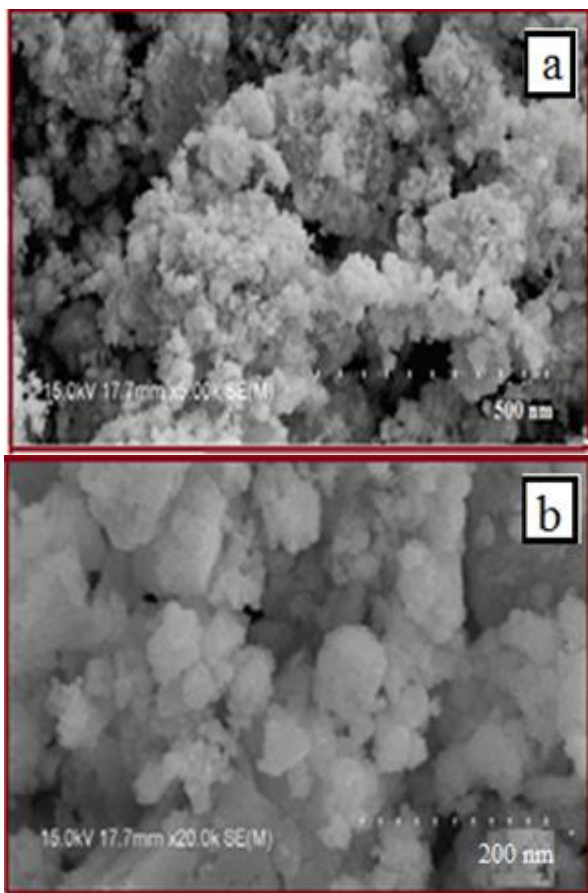


Fig. 5. SEM images of nanocrystals (a) pure PbO (b) Zn doped PbO.

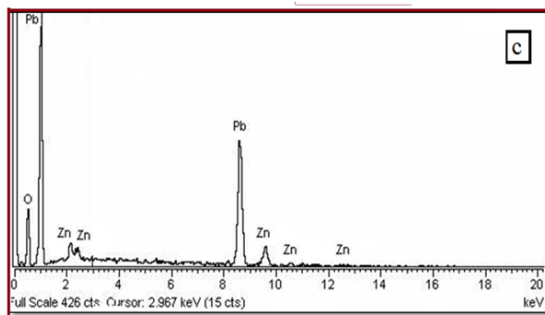


Fig. 5c. EDS spectrum of Zn doped PbO nanocrystals.

## 5. Conclusion

Zn doped PbO nanocrystals have been successfully synthesized by chemical method. Lighter Zn atoms with smaller ionic radius can be easily incorporated into the PbO matrix during the synthesis without any distortion in the lattice structure. An optimum concentration 0.1 M of Zn has been found to be more effective in yielding PbO nanocrystals with defined crystallinity and smaller size of about 23 nm. PL studies showed improved band gap energy and reduced defects such as oxygen vacancies were also achieved. Zn doped PbO nanocrystals with modified

structural and optical characteristics can be effectively utilized in the fabrication of sensor devices.

## Acknowledgement

The author (N.M) wishes to thank the Department of Science and Technology, New Delhi, India for the financial support (DST-Inspire fellowship).

## References

- [1] W. J. Jaffe, R. Cook, H. Jaffe, Piezoelectric ceramics, New York: Academic press (1971).
- [2] M. E. Lines, A. M. Glass, Principles and applications of ferroelectrics and related materials, Oxford, UK:Oxford university presses (2001).
- [3] J. F. Scott, sci. **315**, 954 (2007).
- [4] T. Aoki, Hatanaka, D. C. Look, Appli. Phys. Lett. **76**, 3257 (2000).
- [5] M. S. Nisari, F. Mohandes, F. Davar, Polyhed. **28**, 449 (2009).
- [6] Y. L. Wu, A. I. Y. Boey, X. T. Zeng, X. H. Zhang, Appli. Surf. Sci. **253**, 5473, (2007).
- [7] S. Gnanam, V. Rajendran, Inter. J Nanomater. Biostructures, **1**(2), 12 (2011).
- [8] D. Sridevi, K. V. Rajendran, Bullet. of Mater. Sci., **32**, 165 (2009).
- [9] T. B. Light, J. M. Eldrige, J. W. Matthews, J. H. Greiner, J. appli. phys. **46**, 1489 (1975).
- [10] Mashkoor Ahmad, Caofeng Pan, Wang Yan, Jing Zhu, Mater. Sci. engine. B, **174**, 55 (2010).
- [11] Dewei Chu, Yuping Zeng, Dongliang Jiang, Mater. Resear. Bull. **42**, 814 (2007).
- [12] K. Vanheusdon, W. L. Warren, J. A. Voigt, C. H. Seager, D. R. Tallant, Appli. Phys. Lett. **67**, 1280 (1995).
- [13] Ramin Yousefi, Farid Jamali-Sheinin, Abdolhossain Saaedi, Khorsand Zak, Mohsen Cheraghizade, Siamak Pilban-Jahromi, Nay Ming Huang, Ceram. Internatio. 2013.
- [14] S. S. Nath, D. Chakdar, G. Gope, R. Bhattacharjee, J. nanotech. online (DOI 10, 2240/azojono0129).
- [15] M. NowsathRifaya, T. Theivasanthi, M. Alagar, J. nanosci. Nanotech. **2**(5), 134 (2012).
- [16] Sk. Khadeer Pasha, K. Chidambaram, L. John Kennedy, J. JudithVijaya, Sensors sens. Transducers. **122**, 11 (2010).
- [17] G. Westin, M. Nygren, J.mater. sci. **27**, 1671(1992).
- [18] S. Mohammad Jaffar, G. Najmeh, R. Fatemeh,Inorgan. Chim. Act. **396**, 149 (2013).
- [19] M. Kowshik, W. Vogel, J. Urban, S. K. Kulkarni, K. M. Paknikar, Adv. Mater. **14**, 815 (2002).

\*Corresponding author: arulsheelphy@gmail.com